JOURNAL OF THERMOPHYSICS AND HEAT TRANSFER
Vol. 23, No. 2, April–June 2009

Thermodynamic Nonequilibrium in Ice-Slurry Systems

A. Jamil, T. Kousksou,* Y. Zeraouli, and J-P. Dumas
Laboratoire de Thermique Energétique et Procédés, 64013 Pau Cedex, France

DOI: 10.2514/1.39184

Compared with classical secondary refrigerant loops that continuously supply cold energy, ice-slurry systems rely on the use of storage tanks designed to store and supply the cold energy on demand; thus cutting off cooling peak demands. To reliably operate an ice-slurry cooling system, it is very important to know the ice-loading fraction within the ice-slurry storage tank and in the slurry transmission piping. In this paper we compare two ways to measure the local ice fraction inside the storage tank. The first method is based on a direct measure of the ice-slurry temperature, and the second one applies the differential scanning calorimetry technique.

Nomenclature

a	=	antifreeze
i	=	initial
ic	=	ice
m	=	mass, kg
T	=	temperature, K
T_c	=	extrapolated peak onset temperature, K
T_{end}	=	extrapolated end temperature, K
T_f	=	initial peak temperature, K
T_i	=	end peak temperature, K
T_{peak}	=	peak maximum temperature, K
T_{plt}	=	plate temperature of differential scanning calorimetry, K
W	=	mass fraction, kg/kg
β	=	heating rate, $\text{K} \cdot \text{min}^{-1}$

I. Introduction

RECENTLY, ice slurries composed of small ice crystals, water, and an additive (usually ethylene glycol or ethanol) have been studied as a result of the development of indirect-refrigeration systems [1–8]. Ice slurry offers the potential of significantly reducing the energy consumption and emission of greenhouse gases that are caused by air-conditioning installations. The advantages of ice slurries over chilled-water storage and distribution systems include the ability to provide a much higher heat transfer density (due to latent ice), which can lead to much lower flow rates and pumping power, when compared with chilled-water or other single-phase secondary distribution systems.

To reliably operate an ice-slurry cooling system, it is very important to know the ice-loading fraction found in the ice-slurry storage tank and in the slurry transmission piping. As ice slurry consists of a solid and a liquid phase, it is difficult to measure ice mass fraction for a desired accuracy. For ice slurry, there is often a density difference between the two phases, which contributes to the difficulties in measuring ice mass fraction. Several measurement approaches [9–11] based on the difference between conductivity (or specific volume) of water and ice have been investigated and developed. Stamatiou et al. [12] and Ayel et al. [13] have presented some experimental methods that measure the ice-fraction distribution measurements in horizontal pipes or channels, as well as in vertical ducts. In one method, an ice-slurry sample was removed by a sampling probe that was passed through a custom-made online calorimeter unit. It was instrumented and properly calibrated to determine the local ice fraction. An interesting method has been developed by Ayel et al. [13] that measures the antifreeze mass fraction in an aqueous solution by applying supercooling phenomenon. Their method is based on the analysis of the temperature evolution of a small sample of ice slurry during cooling. They exploit the sudden temperature increase that occurs with the appearance of the first crystals. This method is only valid if the antifreeze mass fraction is low.

The storage of ice slurry in tanks is complicated because under certain little-understood conditions, the ice particles progressively grow together, or agglomerate, over time. This makes pumping the slurry out of the tank very difficult, if not impossible. A few reports have been published about the measurement of temperatures and local ice mass fraction of the ice slurry in a storage tank. Bel et al. [14] have examined the temperature distributions in the storage tank. They showed heavy stratification with another distribution of ice concentrations. In several of the works, it is assumed that the liquid and solid phases are in thermodynamic equilibrium. Simultaneous measurements of the mixture temperature distributions and the ice-concentration fields during melting have shown that the thermal equilibrium between the carrier fluid and the ice particles is not always obtained [15,16].

No reliable procedure has yet been developed to measure the ice mass fraction within the storage tank. A method for measuring the presence and progression of ice-particle agglomeration in a storage tank is needed. It is also noteworthy that during the discharge period, the binary mixture melts nonisothermally. The natural convection in the liquid region is double-diffusive in nature (as a consequence of concentration and temperature gradients prevailing in the melting domain) [17,18]. As melting proceeds, the solute is rejected from the crystal particles found in the liquid region. On a local scale, the solute is redistributed by diffusion transport. However, on a macroscopic scale, thermosolutal convection currents carry the expelled solute further away from the site of rejection. This interaction between the melting process and a thermosolutal convection can influence the thermal equilibrium between the solid and liquid phases in the storage tank.

The purpose of the program described in this paper is to develop a method to measure the ice mass fraction at different points inside the storage tank. The information being developed will facilitate the use of the ice storage tank. A comparison between concentrations is determined by using differential scanning calorimetry (DSC). A direct measure of the mixture's temperature is also presented and discussed.

II. Binary-Phase Diagram

Figure 1 presents the equilibrium-phase diagram [21] for a water–ethanol solution, which has an eutectic temperature and concentration of $T_E = -118°\text{C}$ and $W_E = 0.935$. In our application, the eutectic point and overeutectic part are not of interest.

Received 18 June 2008; revision received 10 November 2008; accepted for publication 11 November 2008.

*Avenue de l'Université, B.P. 1155, tarik.kousksou@univ-pau.fr.

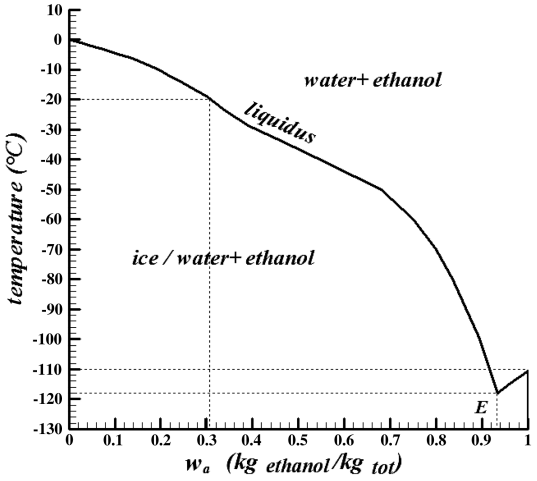

Fig. 1 Phase diagram of the aqueous binary solution of ethanol.

Applying the equilibrium thermodynamic assumption, the ice mass fraction can be evaluated from the mixture's temperature T, which is a function of the ethanol mass fraction W_a in the residual liquid solution:

$$T = T(W_a) \tag{1}$$

Once the initial mass fraction of ethanol in the binary-mixture solution before freezing $W_{a,i}$ and the mixture's temperature T are known, the equilibrium ice mass fraction can easily be calculated from the following equation:

$$W_{\text{ic}}(T) = 1 - \frac{W_{a,i}}{W_a(T)} \tag{2}$$

where $W_a(T)$ is found from the liquidus curve, the inverse of Eq. (1).

Figure 2 shows the thermodynamic relationship existing between the temperature, initial solute concentration, and ice mass fraction for an ethanol–water mixture. Upon close examination of this figure and according to Fournaison et al. [19] and Guilpart et al. [20], it can be concluded that the determination of the ice concentration from the direct measurement of the temperature would yield great uncertainties in the ice mass-fraction values, especially at low ethanol concentrations. The initial solute concentration also has a major impact on the ice-fraction uncertainty.

III. Experiment

A. Experimental Apparatus of the Ice-Slurry System

A schematic diagram of the experimental apparatus is shown in Fig. 3. The apparatus incorporates three components of a secondary

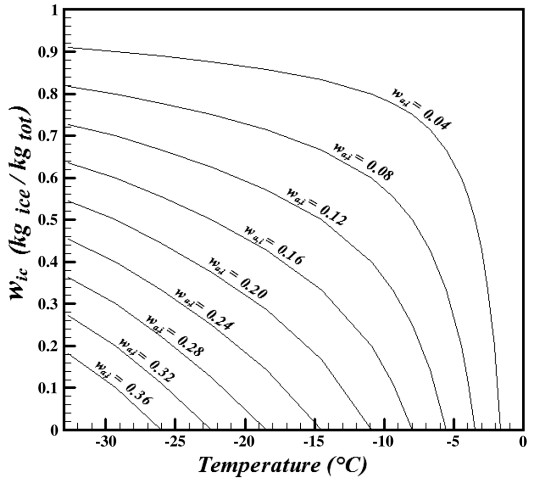

Fig. 2 Ice concentration versus temperature and solute concentration for ethanol–water mixtures.

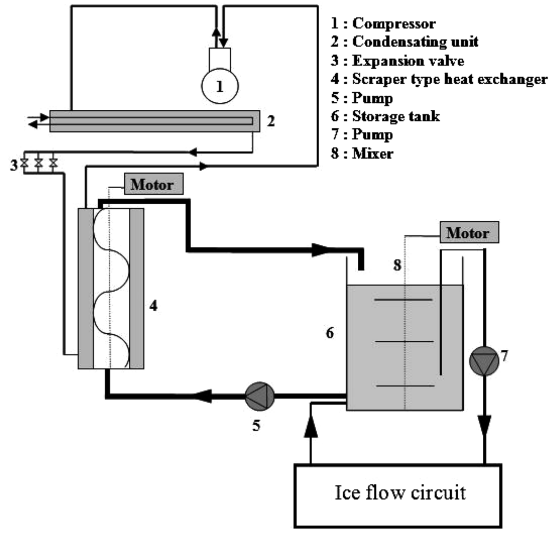

Fig. 3 Schematic diagram of experimental apparatus.

cooling cycle (production, storage, and transport). The conventional scraped-type exchanger generates fine ice crystals with diameters of about 0.1 mm. Ice-slurry storage is basically an open insulated system tank with about a 130-liter capacity with a variable-speed agitator. Ice slurry is transported into the heat exchanger by means of pumping. The main components of the measurement cycle are a volumetric pump and a Rosemound Elite 200 mass flowmeter, which measures the mass flow rate and the density of the binary mixture.

Experiments were performed by producing ice slurry in a storage tank containing an aqueous solution of $W_{a,i} = 0.10$ by weight in an ethanol-in-water solution using a 7 kW refrigerating-capacity scraped-surface ice-slurry generator.

B. Ice-Filtration Method

Initially, ice slurry was produced by using the generator and was stored in the storage tank. As the generator continued to produce ice particles, the ice fraction in the storage tank increased. Once the percentage of ice fraction in the storage tank reached a desired value (above 25%), the slurry-generation system was shut down. About 5 min later, ice-slurry temperature in the storage tank was measured by using DSC analysis or the thermocouple probe.

The mixture samples were taken and directly filtered through a filter in the storage tank (Fig. 4). The size of the filter pores was selected to separate the solution into small ice particles. The filter component was also equipped with a thermocouple to measure the sample temperature (Fig. 5). This temperature was compared with the equilibrium temperature obtained from the DSC analysis of the solution that was passed through the filter.

Given the rapid evaporation of ethanol when exposed to room temperature, all samples were quickly conditioned in tight bottles and transported to a climate chamber to be kept for further processing.

C. Differential Scanning Calorimeter

Thermal analyses of the samples were carried out using the PYRIS Diamond DSC by PerkinElmer. The principle of power compensation used in DSC is widely detailed in [21–23]. It should be remembered that when using a DSC, the calibrations of the temperature and of the heat are very important. Calibration is accomplished by running standard material (usually indium) and comparing the experimental melting point and the enthalpy of transition (or latent heat) with standard values. Two screws in the instrument, one for adjusting temperature readings and the other for adjusting enthalpy readings, were turned until the temperature and enthalpy values were reproducible within the desired tolerance of the standard values. This calibration is important to accurately collect the equilibrium temperature data required for this study.

Because the technique used to predict the ice mass fraction of the sample is based on the DSC analysis, it is useful to list some known

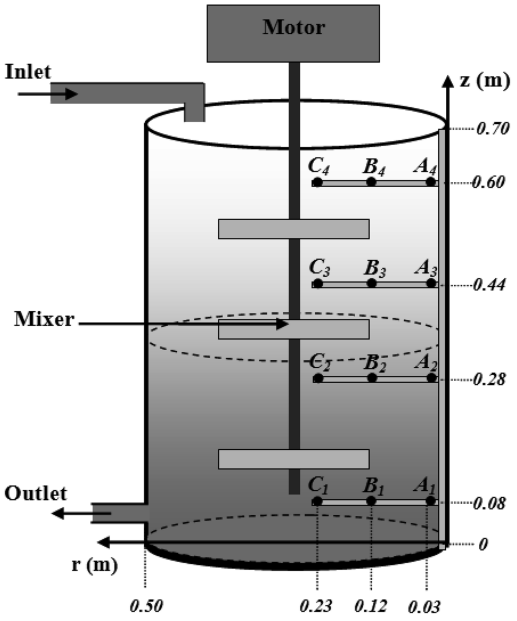

Fig. 4 Storage tank with a mixing element.

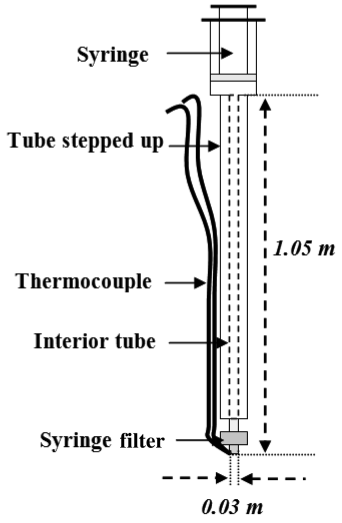

Fig. 5 Filter component.

characteristics of the DSC curve. Usually, the characteristic temperatures taken from DSC measurements are the initial peak temperature T_f, the extrapolated peak onset temperature T_c, the extrapolated end temperature T_{end}, the maximum peak temperature T_{peak} and the end peak temperature T_i [24,25]. All of these are shown in Fig. 6. The use of these temperatures is recommended for both the melting and freezing peak characteristics. The extrapolated peak onset temperature is defined as the intersection between the tangent to the maximum rising slope of the peak and extrapolated sample baseline. T_{peak} represents the value of the plate temperature when the energy exchange is maximum, and T_{end} corresponds to the end of the progressive melting within the sample.

The DSC experiments were conducted by placing each sample in the aluminum DSC cell of a height of $Z_0 = 1.1$ mm and a radius of $R = 2.125$ mm. The sample was cooled at various rates β (between 1 and 20°C/ min) until ice formed in the solution. This was typically at −50°C (observed as a sharp exothermic peak in the DSC thermogram) and it was maintained at this temperature for 3–5 min. The sample was then heated at various scan rates (β from −50 to 10°C) to obtain the thermograms.

In our previous work [1], we presented a DSC study and a theoretical model of the nonisothermal melting of ice slurry in a small

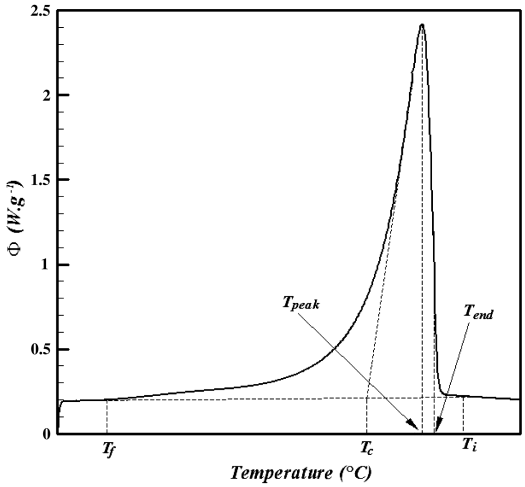

Fig. 6 DSC curve.

container. The influences of both the initial antifreeze mass and the heating rate were investigated. We proposed a DSC technique to detect the solid–liquid equilibrium temperature of the initial mixture before freezing.

For various heating rates, we have shown that all points on the thermograms (for which the abscissa are T_{end}) form a straight line $L_{T_{\text{end}}}$. This cuts the axis of abscissas to T_{plt} (temperature of the DSC plate) (Fig. 7). This temperature corresponds exactly to the equilibrium temperature of the initial mixture T_{eq}.

The same result is obtained for T_{peak}. We have found that for different heating rates, all points for which the abscissa is T_{peak} are aligned. The line $L_{T_{\text{peak}}}$ formed by these points also cuts the axis of abscissas to T_{plt}.

These observations can be explained by the fact that the more the heating rate decreases and comes near to zero, the more the gradients of temperature within the sample become negligible [1]. For lower heating rates ($\beta \to 0$), the end point of the phase transformation practically corresponds to the maximum peak. So the intersection of the two lines $L_{T_{\text{end}}}$ and $L_{T_{\text{peak}}}$ given on the axis of the abscissa indicates the limit of the thermograms (when $\beta = 0$) and it coincides with the equilibrium temperature of the initial mixture for $W_{a,i}$.

By means of the characteristic temperatures of the DSC curves, we can determine the equilibrium temperature of the removed sample. Once the equilibrium temperature of the removed sample and the initial mass fraction of ethanol are known, ethanol mass fraction and ice mass fraction $w_{\text{ice,DSC}}$ can be evaluated by using both the solid–liquid equilibrium-curve relationship (Fig. 1) and Eq. (2).

This technique of analysis was validated in previous works [1,25] by applying it to two binary mixtures: ice/water–ethanol and ice/water–NH_4CL. We have found that the results obtained using this technique coincide perfectly with the data provided by current research.

D. Experimental Uncertainty

Uncertainty estimates for the measurements are based on a propagation-of-error analysis. The principle measurement in the present study is ice mass fraction. However, possible sources of inaccuracy are linked to the measurement of the ice-slurry variables: $W_{a,i}$, $W_a(T)$, and T. The uncertainty of $W_{a,i}$ measurements is evaluated as follows [26,27]:

$$W_{a,i} = \frac{m_{a,i}}{m_{a,i} + m_{\text{water}}} \tag{3}$$

$$\Delta W_{a,i} = \frac{m_{\text{water}}\Delta m_{a,i} + m_{a,i}\Delta m_{\text{water}}}{m_{a,i}(m_{a,i} + m_{\text{water}})} \tag{4}$$

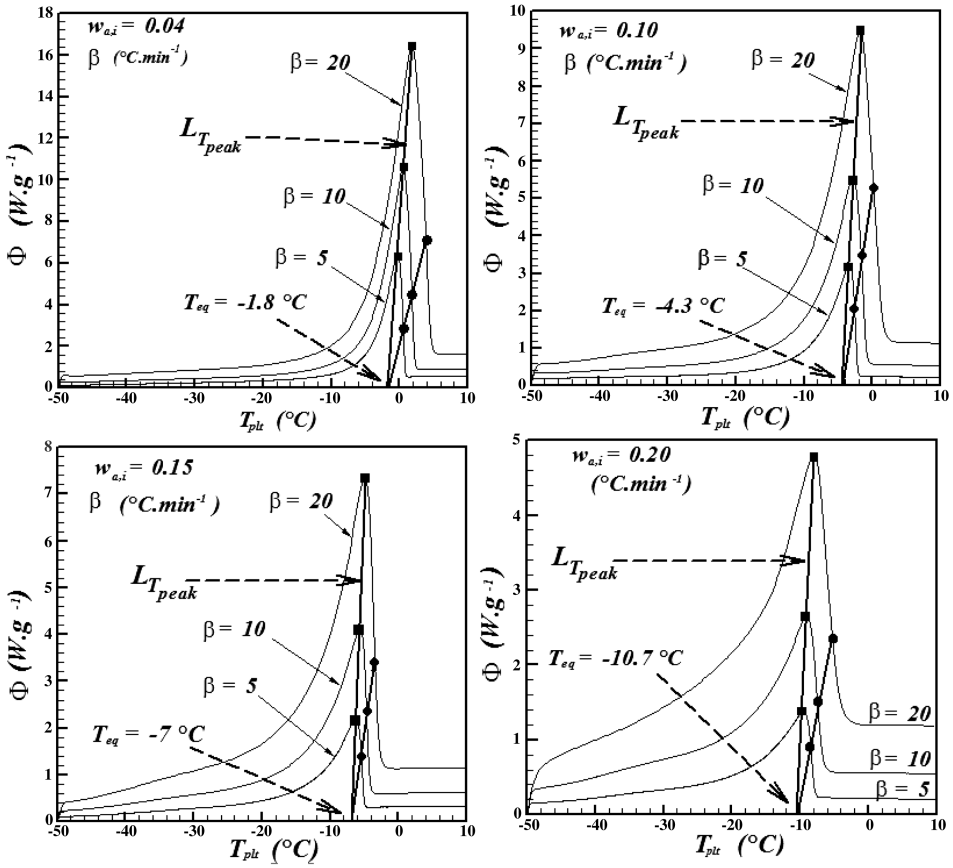

Fig. 7 Determination of equilibrium temperature for various initial antifreeze mass fraction.

where $\Delta m_{a,i}$ and Δm_{water} (respectively, 0.02 and 0.01 g) are the resolution of the water and antifreeze weighing devices, respectively. One can assume thermodynamic equilibrium $W_a(T)$, because it is given by the freezing curve [28]. Using Eq. (4) for the error calculation of each antifreeze concentration shows that the error related to $W_a(T)$ never exceeds 1.5% and becomes negligible for $W_{a,i}$ over 0.15.

Using Eq. (2), the uncertainty of the W_{ic} measurement is evaluated as follows:

$$\frac{\Delta W_{\text{ic}}(T)}{W_{\text{ic}}(T)} = \frac{\Delta W_{a,i}}{W_{a,i}} + \frac{\Delta W_a(T)}{W_a(T)} \tag{5}$$

According to Fournaison et al. [19], for the lowest antifreeze concentrations, the most significant source of error is the evaluation of the initial antifreeze concentration $W_{a,i}$. At a higher antifreeze mass fraction, the error in the measurement of ice-slurry temperature is dominant.

We note that the maximum random uncertainties of the temperature determined directly by using thermocouple and by DSC analysis are, respectively, 0.1 and 0.2%. The latter uncertainties were established from the bench-scale calibration tests [24]. To estimate the repeatability of the experiment, some of the cases were repeated under the same operating conditions. The difference was found to be less than 2%. The error in the location of the thermocouples in the storage tank was determined from in situ calibrations to be about 0.50 mm.

IV. Experimental Results

A. Melting Process Inside the Storage Tank

To describe the heat transfer during the melting process of ice slurry, various thermocouples have been placed at different positions within the storage tank (Fig. 4). To eliminate the effect of the mixer, the storage tank is studied without a mechanical agitator.

Figure 8 illustrates the variation of the temperatures during the melting process in the tank. As can be seen, the melting process is displaced from the wall surface to the center and from the bottom to the upper parts of the tank. If no mixing is applied, the ice slurry in the tank undergoes full stratification. This is due to the buoyancy of the ice particles. This stratification causes a nonuniform ice-concentration profile within the tank. Therefore, the temperature in the upper region is lower than that in the lower region.

In a mechanically agitated tank, ice particles can be damaged by collision with the stirrer blade. This collision subdivides the parent crystal into a number of smaller pieces with a wide spectrum of sizes [29]. In a perfectly agitated storage tank the ice-slurry temperature remains relatively constant. The solid–liquid equilibrium-curve relationship and the mixture's temperature can be used to evaluate the ice content within the mixture [20].

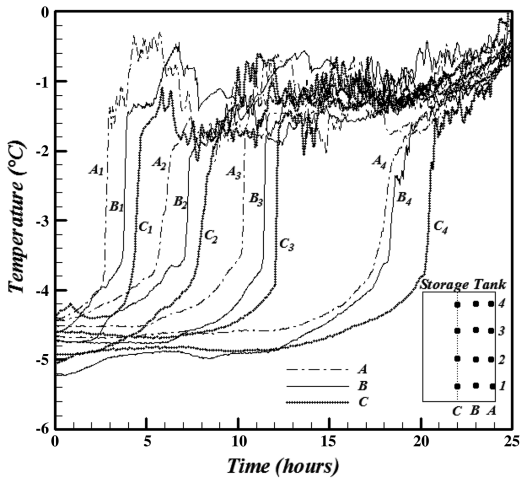

Fig. 8 Evolution of the temperatures in the tank as a function of time.

As melting continues, the volume of ice particles decreases and the remaining ice particles float to the upper surface to form a packed bed (see Fig. 8). The exchange between the floating packed bed and the solution located in the lower part of the storage tank is carried out both by conduction and convection.

Because there are more water molecules in the upper region than in the lower one, there is obviously a transfer of ethanol molecules from the lower to the upper part of tank. This is a result of random molecular motions.

B. Ice Mass-Fraction Measurements

Just after the shutdown of the slurry-generation system (after about 5 min), the storage tank was studied in two situations: with mechanical agitation and without it. The ice-slurry temperature profile was obtained by using a syringe inserted at different positions inside the tank (see Fig. 4).

Figures 9 and 10 present the ethanol mass fraction obtained from the two temperatures: the equilibrium temperature (calculated from the DSC analysis) and the mixture temperature (measured by the thermocouple). In this work, we present only the ice-slurry temperatures at $r = 12$ cm.

The dashed line represents the solid–liquid equilibrium-curve relationship, where z is the distance from the bottom of the tank. The results indicate that the ethanol concentrations determined by DSC analysis $w_{a,\mathrm{DSC}}$ are lower than those obtained by the direct measure of temperature $w_{a,T}$. The difference between $w_{a,T}$ and $w_{a,\mathrm{DSC}}$ is especially noticeable in the bottom part of the tank and chiefly when the mechanical agitator is not applied. We can also note that the thermodynamic equilibrium does not occur at any point in the accumulation tank. As discussed earlier, the kinetics of the ice melting and the molecular diffusion are the most important phenomena that influence the measurement of the ethanol concentration. In fact, during the melting process, the heat that is transferred from the solution to the ice particles can be divided into two types. One is the melting latent heat (which causes fusion on the surface) and the other is heat conduction from the surface into the ice (which raises the internal temperature). This process causes a nonthermal equilibrium between the solution and the melting solid particles. On the other hand, the molecular diffusion of the water (which is derived from the melting particles) in the surrounding solution is slower, because the ethanol concentrations $w_{a,T}$ obtained from the direct measure of temperature are lower than those determined by DCS. The clear nonlinearity in the graphs between the points $z = 15$ and 25 cm can be ascribed to the random molecular motions inside the tank.

Figures 9 and 10 also indicate that the temperature measured by the thermocouple does not correspond to the equilibrium temperature, as a thermal equilibrium between the solution and the ice particles is not always obtained during melting.

To compare the ice concentrations $w_{\mathrm{ice},T}$ obtained from the direct measure of the mixture temperature and those determined by the DSC technique $w_{\mathrm{ice,DSC}}$, we have calculated the relative error at different positions of the tank:

$$\text{error} = \frac{|w_{\mathrm{ice,DSC}} - w_{\mathrm{ice},T}|}{w_{\mathrm{ice,DSC}}} \tag{6}$$

Figures 11 and 12 illustrate the relative error versus the height of the storage tank. They clearly show the basic difference between $w_{\mathrm{ice,DSC}}$ and $w_{\mathrm{ice},T}$. The results also indicate that the relative error is very high in the lower part of the storage tank. This can be explained by the fact that in the lower region, the ice-fraction measurement is influenced by various phenomena such as the suspension of ice particles, the melting process, and molecular diffusion.

Because the melting process occurs continuously in the top region of the tank, the mixture temperature remains relatively constant. This temperature depends mainly on the initial ethanol concentration and the ice mass fraction. Because the relative error is lower in the upper region of the storage tank, the ethanol mass fraction can be evaluated from the DSC technique.

The direct measure of the mixture temperature to predict the ice mass fraction is only highly accurate when the storage tank is perfectly stirred. Without mechanical agitation, it is impossible to use a temperature-measurement device to determine the ice concentration in the storage tank. The ice-slurry segregation phenomenon, which is due to ice-buoyancy effects in the storage tank, would cause

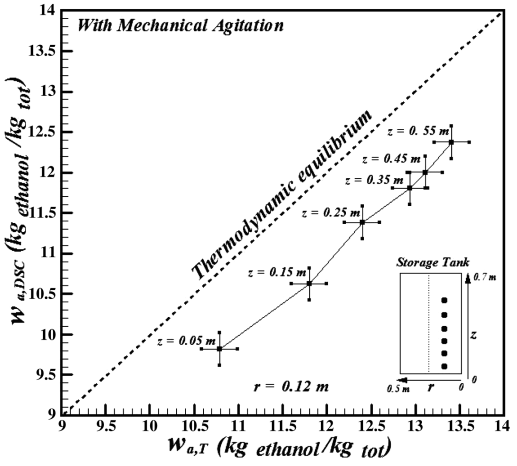

Fig. 9 Ethanol mass fraction inside the tank (without mechanical agitation).

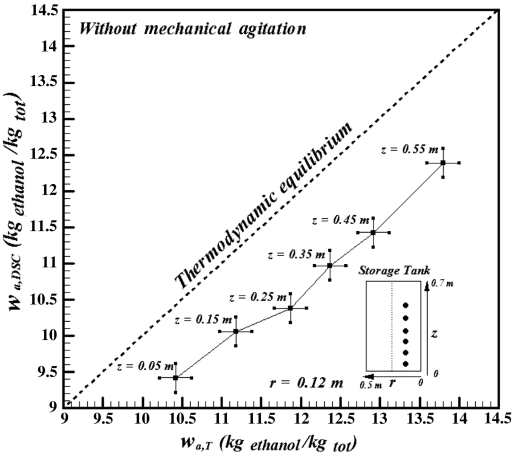

Fig. 10 Ethanol mass fraction inside the tank (with mechanical agitation).

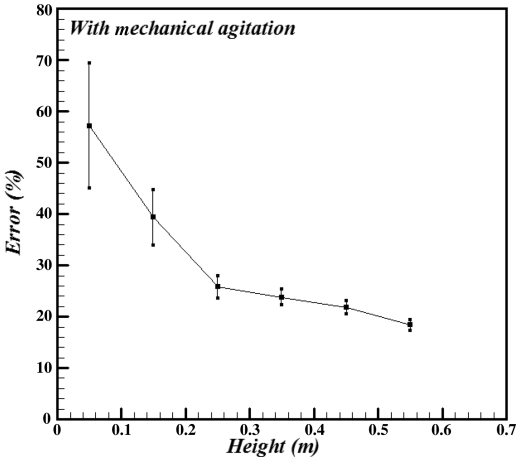

Fig. 11 Relative error of ice-concentration measurement: tank with mechanical agitation.

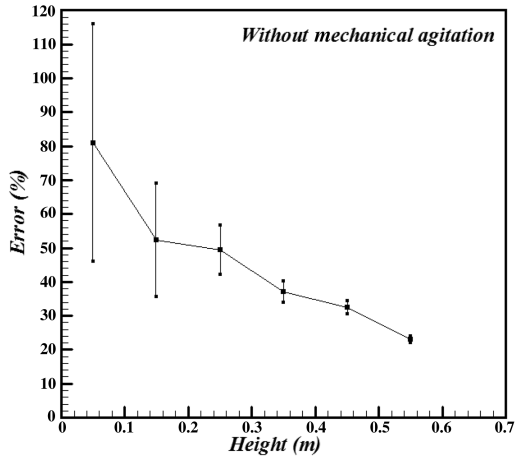

Fig. 12 Relative error of ice-concentration measurement: tank without mechanical agitation.

a variation in the solute concentration of the residual liquid. This would adversely affect the temperature measurement and, consequently, ice-fraction accuracy.

The suspension of ice particles, the melting process, and the molecular diffusion have a significant effect on ice-concentration measurement. These phenomena should be considered when the probe is used to measure the concentration of the solids.

V. Conclusions

An experimental technique has been developed to measure the local ice mass fraction within ice-slurry systems. It has been found that the thermodynamic equilibrium does not occur at any point in the accumulation tank during the melting process.

The direct measurement of the ice fraction is very difficult to conduct because of the instability of the slurry. Indeed, it is susceptible to melt and to sediment during experimentation. It would be interesting to carry out this study for storage tanks of different sizes. Experimental work and theoretical calculations will be important to investigate natural convection and molecular diffusion inside the storage tank during the melting process.

References

[1] Kousksou, T., Jamil, A., Zeraouli, Y., and Dumas, J. P., "Equilibrium Liquidus Temperatures of Binary Mixtures from Differential Scanning Calorimetry," *Chemical Engineering Science*, Vol. 62, No. 23, Dec. 2007, pp. 6516–6523. doi:10.1016/j.ces.2007.07.008

[2] Grandum, S., Yabe, A., Tanaka, M., Takemura, F., and Nakagomi, K., "Characteristics of Ice Slurry Containing Antifreeze Protein for Ice Storage Applications," *Journal of Thermophysics and Heat Transfer*, Vol. 11, No. 3, 1997, pp. 461–466. doi:10.2514/2.6262

[3] Egolf, P. W., and Kauffeld, M., "From Physical Properties of Ice Slurries to Industrial Ice Slurry Applications," *International Journal of Refrigeration*, Vol. 28, No. 1, Jan. 2005, pp. 4–12. doi:10.1016/j.ijrefrig.2004.07.014

[4] Kauffeld, M., Kawaji, M., and Egolf, P. W., "Handbook on Ice Slurries: Fundamentals and Engineering," *International Journal of Refrigeration*, Vol. 1, Jan. 2005, pp. 360.

[5] Shukla, A., and Prakash, A., "Ultrasonic Technique to Determine Particle Size and Concentration in Slurry Systems," *Chemical Engineering Science*, Vol. 61, No. 8, Apr. 2006, pp. 2468–2475. doi:10.1016/j.ces.2005.11.027

[6] Egolf, P. W., Sari, O., Meilli, F., Moser, P., and Vuarnoz, D., "Heat Transfer of Ice Slurries in Pipe," *International Journal of Refrigeration*, Vol. 28, Sept. 1999, pp. 106–123.

[7] Sari, O., and Egolf, P. W., "Viscosity Applied to the Bingham Substance Ice Slurry," *Second Workshop on Ice Slurries*, International Inst. of Refrigeration, Lucerne, Switzerland, 2006, pp. 68–80.

[8] Stamatiou, E., and Kawaji, M., "Thermal and Flow Behavior of Ice Slurries in Vertical Rectangular Channel, Part 2: Forced Convective Melting Heat Transfer," *International Journal of Heat and Mass Transfer*, Vol. 48, No. 17, Aug. 2005, pp. 3544–3559. doi:10.1016/j.ijheatmasstransfer.2005.03.019

[9] Kakka, R. S., "Review of Instruments for Measuring Flow Rate and Solids Concentrations in Steel Works Slurry Pipelines," *Hydrotransport 3*, BHRA Fluid Engineering, Cranford, England, U.K., 1974, pp. 81–92.

[10] Nasr-El-Din, H., Shook, C. A., and Colwell, J., "A Conductivity Probe for Measuring Local Concentrations in Slurry Systems," *International Journal of Multiphase Flow*, Vol. 13, No. 3, May–June 1987, pp. 365–378. doi:10.1016/0301-9322(87)90055-3,

[11] Stamatiou, E., and Kawaji, M., "Thermal And Flow Behavior of Ice Slurries in Vertical Rectangular Channel, Part 1: Local Distribution Measurements in Adiabatic Flow," *International Journal of Heat and Mass Transfer*, Vol. 48, No. 17, Aug. 2005, pp. 3527–3543. doi:10.1016/j.ijheatmasstransfer.2005.03.020

[12] Stamatiou, E., Kawaji, M., and Coldstein, V., "Ice Fraction Measurements in Ice Slurry Flow Through a Vertical Rectangular Channel Heated from One Side," *Proceedings of the Fifth Workshop on Ice Slurries*, edited by P. W. Egolf, International Inst. of Refrigeration, Stockholm, 2002.

[13] Ayel, V., Lottin, O., Popa, E., and Peerhossaini, H., "Using Undercooling to Measure the Freezing Points of Aqueous Solutions," *International Journal of Thermal Sciences*, Jan. 2005, Vol. 44, No. 1, pp. 11–20. doi:10.1016/j.ijthermalsci.2004.04.012

[14] Bel, O., and Lallemand, A., "Study of a Two Phase Secondary Refrigerant 1: Intrinsic Thermophysical Properties of an Ice Slurry," *International Journal of Refrigeration*, Vol. 22, No. 3, May 1999, pp. 164–174. doi:10.1016/S0140-7007(98)00070-X

[15] Egolf, P. W., Kitanovski, A., Ata-Caesar, D., Stamatiou, E., Kawaji, M., Bedecarrats, J. P., and Strub, F., "Thermodynamics and Heat Transfer of Ice Slurries," *International Journal of Refrigeration*, Vol. 28, No. 1, Jan. 2005, pp. 51–59. doi:10.1016/j.ijrefrig.2004.07.015

[16] Mellan, I., *Industrial Solvents Handbook*, Noyes Data Corp., Park Ridge, NJ, 1977, pp. 133.

[17] Chakraborty, S., and Dutta, P., "Effects of Solid Layer Thickness and Nominal Composition on Double-Diffusive Instabilities During Solidification of Binary Alloy Cooled from the Top," *International Journal of Heat and Mass Transfer*, Vol. 47, No. 1, Jan. 2004, pp. 185–190. doi:10.1016/S0017-9310(03)00383-1

[18] Kumar, P., Srinivasan, K., and Dutta, P. "Visualization of Convection Loops due to Rayleigh-Benard Convection During Solidification," *Mechanics Research Communications*, Vol. 33, No. 5, 2006, pp. 593–600. doi:10.1016/j.mechrescom.2005.08.001

[19] Fournaison, L., Chourot, J. M., Faucheux, M., and Guilpart, J., "Ice Fraction Error Calculation in Ice Slurries," *Proceedings of the Third IIR Workshop on Ice Slurries*, Horw, Lucerne, Switzerland, and International Inst. of Refrigeration, Paris, 16–18 May 2001, pp. 35–42.

[20] Guilpart, J., Stamatiou, E., and Fournaison, L., "The Control of Ice Slurry Systems: An Overview," *International Journal of Refrigeration*, Vol. 28, No. 1, Jan. 2005, pp. 98–107. doi:10.1016/j.ijrefrig.2004.07.007

[21] Dumas, J. P., Zeraouli, Y., and Strub, M., "Heat Transfer Inside Emulsions: Determination of the DSC Thermograms, Part 2: Melting of the Crystallized Droplets," *Thermochimica Acta*, Vol. 236, May 1994, pp. 239–248. doi:10.1016/0040-6031(94)80272-6

[22] Jamil, A., Kousksou, T., Zeraouli, Y., Gibout, S., and Dumas, J. P., "Simulation of the Thermal Transfer During an Eutectic Melting of a Binary Solution," *Thermochimica Acta*, Vol. 441, No. 1, Feb. 2006, pp. 30–34. doi:10.1016/j.tca.2005.11.010

[23] Kousksou, T., Jamil, A., Zeraouli, Y., and Dumas, J. P., "DSC Study and Computer Modeling of the Melting Process in Ice Slurry," *Thermochimica Acta*, Vol. 448, No. 2, Sept. 2006, pp. 123–129. doi:10.1016/j.tca.2006.07.004

[24] Jamil, A., "Etude Expérimentale et Modélisation de l'Analyse Calorimétrique des Fusions et des Déséquilibres de Phases dans les Coulis de Glace," Ph.D. Thesis, Lab. de Thermique Energetique et Procedes, Pau, France, 2006.

[25] Jamil, A., Kousksou, T., Zeraouli, Y., and Dumas, J. P., "Liquidus Temperatures Determination of the Dispersed Binary System,"

Thermochimica Acta, Vol. 471, No. 1–2, May 2008, pp. 1–6. doi:10.1016/j.tca.2008.02.003

[26] Moffat, R. J., "Describing the Uncertainties in Experimental Results," *Experimental Thermal and Fluid Science*, Vol. 1, Jan. 1988, pp. 3–17. doi:10.1016/0894-1777(88)90043-X

[27] Kline, S. J., and McClintock, F. A., "Describing Uncertainties in Single-Sample Experiments," *Mechanical Engineering*, Vol. 75, No. 1, Jan. 1953 pp. 3–8.

[28] Melinder, A., "Accurate Thermophysical Properties Values of Water Solutions are Important for Ice Slurry Modelling and Calculations," *Third Workshop on Ice Slurries of the IIR*, International Inst. of Refrigeration, Lucerne, Switzerland, 2001, pp. 11–18.

[29] Ponk, P., Hansen, T. M., Ferreira, I. C. A., and Witkamp, G. J., "Time Dependent Behaviour of Different Ice Slurries During Storage," *International Journal of Refrigeration*, Vol. 28, No. 1, 2005, pp. 27–36. doi:10.1016/j.ijrefrig.2004.07.011